

**A Thesis**  
on  
**CaO/MgO effect on the crystallisation and optical properties of  
potassium silicate glasses.**

Submitted in partial fulfil requirements for the award of degree of

**Master of Physics**

Submitted by:

**Jasleen Kaur**

Roll.no. 302004006

Under the supervision of:

**Dr. Kulvir Singh**

**(Professor & Head)**



**School of Physics and Material Science**  
**Thapar Institute of Engineering & Technology**  
**Patiala, Punjab-147004,2022.**

*Accomplished with the blessing*

*Of*

*God*

*&*

*Dedicated to my loving parents*

*S. Baldev singh and Jasveer kaur*

*&*

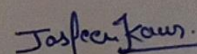
*My lovely sisters and brothers.....*

### CERTIFICATE

I hereby declare that the work which has been presented in the dissertation entitled “CaO/MgO effect on the crystallisation and optical properties of potassium silicate glasses” is an authentic record of my own work carried out for the partial fulfilment of the requirement for the award of the degree of Masters of Science in Physics at Thapar Institute of Engineering & Technology, Patiala (Punjab) under the guidance of **Dr. Kulvir Singh**, (Professor & Head), School of Physics and Materials Science. The matter submitted in this dissertation report has not been submitted in part or full for the award of any other degree.

Date: 27 July 2022

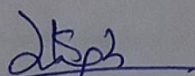
Patiala



Jasleen Kaur

(302004006)

This is to certify that the above statement made by the candidate is correct and true to the best of my knowledge and belief.



**Dr. Kulvir Singh**

Professor & Head

School of Physics and Material Science

Thapar Institute of Engineering & Technology, Patiala – 147004

## **Acknowledgement**

At this momentous occasion of binding my thesis, I would like to acknowledge the contribution of all those benevolent people, I have been blessed to associate with. All the datacollection, theories would have failed to serve their purpose for me if blessings of God would not have joined hands with my efforts.

My first and foremost offering of thanks goes to Dr. Kulvir Singh, School of Physics and Material Science, Thapar Institute of Engineering and Technology, Patiala. He guided me through this path with his positive criticism stimulating discussion and consistence encouragement. His meticulous attention towards my proceedings, his devoted time and his ideas has enabled me to make the project a success. His faith in me has always made me more confident. His blessing always made me optimistic.

I would like to give my special thanks to Trisha Walia for guiding me at various stages of my experimental work. I am also grateful to my dear friends and colleagues at the school of Physics and Material Science.

## CONTENTS

Sr.No.		Page No.
1.	<i>Certificate</i>	i
2	<i>Acknowledgement</i>	ii
3.	<i>List of tables</i>	v
4.	<i>List of figures</i>	vi
5.	<i>Abstract</i>	vii
	<b>Chapter – 1 Introduction</b>	
1.1	Background	1
1.2	Fundamental of glass	1
1.3	Formation of glass	2
1.4	Component of glass	3
	1.4.1 Glass network former	4
	1.4.2 Network Modifier	4
	1.4.3 Intermediates	4
	1.4.4 Colorants and fining agent	4
1.5	Types of oxide glass	4
	1.5.1 Silicate glass	4
	1.5.2 Borate glass	5
	1.5.3 Phosphate glass	5
	1.5.4 Chalcogenide glass	5
1.6	Properties of glass	5
	1.6.1 Optical properties	6
	1.6.2 Structural properties	6
	1.6.3 Thermal properties	7
	1.6.4 Mechanical properties	7
1.7	Glass ceramics	8
	1.7.1 Nucleation	8
	1.7.2 Growth	8
1.8	Properties of glass ceramics	9
	References	10

	<b>Chapter-2</b>	<b>Literature Review</b>	12
		References	19
	<b>Chapter-3</b>	<b>Experimental Details</b>	21
3.1		Sample preparation	21
3.1.1		Preparation of Glass	22
3.1.2		Preparation of glass-ceramic pallets	22
3.2		Characterizations of as quenched/heat-treated samples	22
	3.2.1	X-ray diffraction (XRD)	23
	3.2.2	Raman spectroscopy	24
	3.2.3	UV-visible spectroscopy	25
		References	27
	<b>Chapter- 4</b>	<b>Results and Discussion</b>	28
4.1		X-ray diffraction analysis	28
4.2		Raman Spectra	30
	4.2.1	Effect of Heat treatment	33
4.3		UV Analysis	33
		References	38
	<b>Chapter-5</b>	<b>Conclusion and Future Scope</b>	39
5.1		Conclusion	39
5.2		Future Scope	39

## LIST OF TABLES

Table 3.1: Glass labels along with their compositions in mol% ..... 21

Table 4.1: Crystalline Phases and their volume Fraction formed in present glass-ceramics.....30

Table 4.2: Band gap values of given glass ceramics with their sample code ..... 36

## LIST OF FIGURES

Figure 1.1 Specific volume versus temperature curve for glass and crystalline material.....	3
Figure 3.1 Experimental steps followed in order to study the properties of the given heat treated glasses.....	23
Figure 3.3: Raman Spectroscopy Instrument.....	25
Figure 4.1: XRD pattern of (a) 1 hour heat treated CM series, (b) 10 hour heat treated CM series.....	28-29
Figure 4.2: Raman Spectra of (a) CM0, CM0(1) AND CM0(10), (b) CM10, CM10(1) AND CM10(10), (c) CM20, CM20(1) AND CM20(10) and (d) CM30, CM30(1) AND CM30(10) .....	31-32
Figure 4.3: Tauc's plot for determination of optical band gap of glass-ceramics (a) CM-0, (b) CM-10, (c) CM-20, (d) CM-30.....	34-36

## ABSTRACT

Four potassium silicate with variable calcium and magnesium oxides were synthesized by melt quench technique. The glasses were powdered and then pelletized. The glass pellets were heat treated at 850°C for 1 and 10 hours to convert them into glass ceramics. The heat treated glass-ceramics were characterized by X-ray diffraction, Raman Spectroscopy and UV spectroscopy to check the effect of heat treatment on various properties of glass ceramics. After 1 hour heat treatment, the higher MgO (30mol%) in 55SiO<sub>2</sub>-10K<sub>2</sub>O-5MgO-30MgO containing glasses were converted in glass ceramics and form the Mg<sub>2</sub>SiO<sub>2</sub> phases. The Raman spectra show the remarkable change as glass converted into the glass ceramics and Raman peaks became sharper. The optical band gap was observed in wide band gap semiconductor range.

**1.1 Background**

In 3500 BC, the history of glass formation was uncovered in ancient Egypt. According to archaeological data, the earliest glass was discovered in Egypt and northern Syria. Early in the third millennium BC, beads were the first known glass artefact. It was unintentionally created while working with metal or making faience. It is a vitreous substance created by a glazing-related event.

In 1730 BC, glass materials were first being developed in India. Later, on glass materials were recovered across the Roman Empire and are now used in commercial, household, and funerary settings. Glass was widely employed in Anglo-Saxon times in things like windows, beads, jewellery, and other objects [1].

In the 20th century, glass - such as laminated glass and reinforced glass-were employed as building materials. The telecommunications business has been transformed by the replacement of copper lines with glass optical fibres. The study of nonlinear optical characteristics of glass is promoted for communication. The majority of the time, glasses serve as excellent insulators, although they can be manufactured to have a wide variety of electrical properties. Glasses are being utilised as a sealant in energy technology in addition to the many other uses, they have in all facets of life. The glasses are additionally applied in fuel cells and battery applications as electrolytes [2].

**1.2 Fundamental of glass**

Glasses are generally brittle, rigid, and amorphous in nature. Additionally, Glass exhibits glass transition temperature ( $T_g$ ), which is the point at which it transitions from a solid to a rubbery state. Based on the glass network former the oxide glasses can be classified in three broad categories namely silicate, borate and phosphate glasses.

The majority of silicate glasses are typically transparent, making them useful as window panes in building construction. Because of their reflecting and refractive properties, these glasses can be utilised for optical lenses, prisms, and fine glassware for daily uses.

Additionally, glasses that have been quenched can be properly heated to transform them into glass ceramics. The volume proportion of newly generated crystalline phases alters the glasses' physical characteristics. Therefore, depending on the kinds of produced crystalline phases and their volume fractions in the glass matrix, crystallisation of the glasses may be favourable or unfavourable depending on the application. [3-5].

### **1.3 Formation of glasses**

When a liquid cools slowly, the atoms and molecules have time to arrange themselves in an ordered manner in most of the cases, forming crystals, whereas when a liquid cools quickly, the atoms and molecules arrange themselves in a random manner, which results in the formation of glass following quenching. Additionally, fast cooling rate, other criteria also play an important role to form the glasses [6].

In order to create glass, cooling must occur at a pace greater than crystallisation and below the material's melting point ( $T_m$ ). According to Zachariasen, the constituent of glass should have a low coordination number, the cation coordination number must be less than five. Cations are only linked by two such oxygen atoms and do not form additional bonds with other cations.

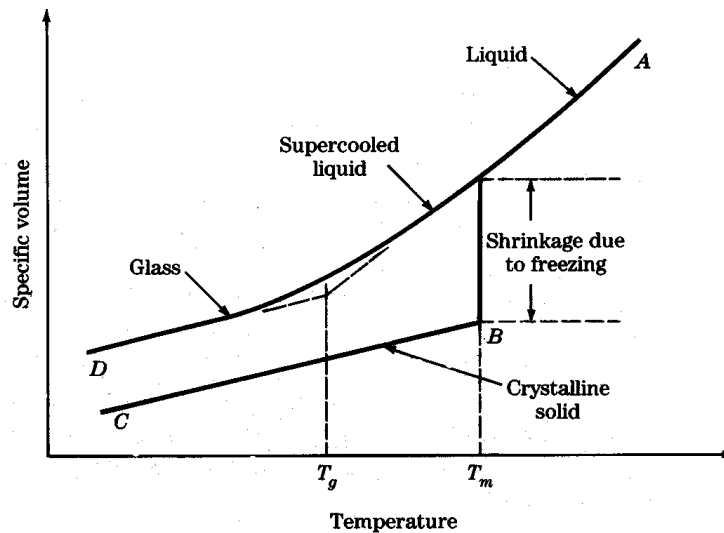


**Figure 1.1** Specific volume versus temperature curve for glass and crystalline material [7].

The specific volume curve with respect to temperature is shown in Fig1.1, together with the glass thermal expansion. The graphical change in slope with temperature or  $T_g$ , is depicted and is highly influenced by the rate of cooling, as indicated by differential thermal analysis (DTA) and differential scanning calorimetry (DSC). The "melt-quench technique" is used in this method. However, many techniques are employed, including glow discharge decomposition, sputtering, and sol-gel methods to synthesis the glasses.

## 1.4 Component of glasses

### 1.4.1 Glass network former

As mentioned in introduction section of this chapter the glass former must have bond energy in certain range with low coordination number. Network formers frequently contain the cations like boron, silicon, germanium, and phosphorus. They can covalently bond with oxygen because they are in a high valence state, which means they have an excess or deficiency of electrons that makes it easy for them to do so. Thus, in oxide glass, silicate, borate and phosphate are the common glass formers [8].

### **1.4.2 Network modifiers**

These oxides exhibit lower bond energy than the glass formers and lower field strength than glass formers. The  $\text{Na}_2\text{O}$ ,  $\text{Li}_2\text{O}$ ,  $\text{K}_2\text{O}$ ,  $\text{CaO}$ ,  $\text{MgO}$  etc act as modifiers in oxide glasses [9].

### **1.4.3 Intermediates**

As the name indicate, these materials can act as former or modifier in the glass depending on their amount in the glass composition. For example,  $\text{TiO}_2$ ,  $\text{Y}_2\text{O}_3$ ,  $\text{Cr}_2\text{O}_3$ ,  $\text{Fe}_2\text{O}_3$ ,  $\text{Al}_2\text{O}_3$  etc are well known intermediates.

### **1.4.4 Colorants and fining agents**

Colorants are used to regulate the colour of glass. Fining agents are introduced to the glass batches during glass production in order to remove air bubbles from the glass melts. Transition metal oxides (3d elements) or 4f rare earths metals are the most common colourants, whereas arsenic oxide,  $\text{NaCl}$ , and  $\text{CaF}_2$  are the most common fining agents. Due to their little addition, these fining agents do not change the characteristics of the glass [10- 11].

## **1.5 Types of oxide glasses**

The glass can be divided into the following categories based on their composition and formers.:

### **1.5.1 Silicate glasses**

Most researched glasses are made of silicates. The basic ingredient is silica in these glasses. The vitreous silica has very high glass transition temperature and required the high melting temperature to form the glass. As the amount of silica in the glass composition varied the properties are also changed. So, those glass composition exhibit the silica as glass former, usually those glasses are called the silicate glasses. Silicate glasses find applications in the telecommunication glass waves, optical devices etc. The silicon and oxygen form a three-

dimensional network link. Alkali and alkaline earth metals are employed as network modifiers to alter the silicon network. Silicate glasses are larger than soda lime glass glasses in comparison. Nearly negligible thermal expansion, large optical band gap, low electrical conductivity, and strong corrosion resistance are some of the general features of the glasses [12].

### **1.5.2 Borate glasses**

The boron oxide ( $B_2O_3$ ) is a different sort of network former. Glasses that use boron oxide as a network forming component are referred to as borate glasses. Borate glasses are primarily employed for their fast ionic conductive characteristics and energy storage applications.

### **1.5.3 Phosphate glasses**

The phosphate-based glasses usually exhibit lower thermal stability and hygroscopic in nature. The primary component of phosphate glasses is  $P_2O_5$ , and because of their time- independent dc conductivity and negative temperature coefficient of resistance, these glasses are mostly used in semiconductor technology and as bio-glass.

### **1.5.4 Chalcogenide glasses**

In recent years, chalcogenide glasses have developed a fascinating and ground-breaking new platform for all optical data processing for photonic devices. Chalcogenide glasses have received a lot of attention, recently, because of its prospective use in biosensors, solar cells, memory devices, fibre optics, and IR photo detectors. Chalcogenide glasses are formed from IV and V group elements. Chalcogenide glasses tend to absorb radiation in the visible spectrum [13-15].

## **1.6 Properties of glasses**

The unique qualities of glasses are connected to their liquid-like composition. Transparency is a characteristic of liquids as opposed to the solid state. Glasses lack internal grain

boundaries and structural components with specified orientations because they are isotropic. Some of the properties of glasses are given in the following section.

### **1.6.1 Optical properties**

Glass lenses to help people with failing vision, glass windows to let light into buildings while protecting them from the elements, glass in lightbulbs to provide light in the dark, and glass fibres for improved communication are among the major technological advancements that have increased the comfort of living. Refractive index, optical dispersion, and infrared spectrum transmission qualities are the foundations for glass fibre communication. Among the most significant technological developments that have raised the standard of living are glass lenses to help people with poor vision, glass windows to let light into buildings while shielding them from the elements, glass in lightbulbs to provide light in the dark, and glass fibres for better communication. The pillars of glass fibre communication are refractive index, optical dispersion, and infrared spectrum transmission properties. With an increase in the composition of oxides like CaO, MgO, ZnO, PbO, and B<sub>2</sub>O<sub>3</sub>, the refractive index has also been seen to rise. In addition to composition, the rate of cooling affects a glass's refractive index. In comparison to well-annealed glass at room temperature, a glass that has been chilled more quickly will have a higher index of refraction [16].

### **1.6.2 Structural properties**

Unique physical and chemical characteristics of glasses and melts depend on temperature, pressure, and chemical make-up. An accurate structural description is necessary to comprehend these characteristics. The irregular nature of glasses and their intricate chemical composition, and melts prevent the creation of a distinctive, crystal-like structure. However, despite the absence of regularity glasses and melts maintain a distinctive short-range order that abides by fundamental crystal-chemical laws, as well as long-range order [17]. However, there is not much information available, explains how temperature, pressure, or both can

affect the local structure of glass. Combining theoretical and experimental methods is necessary to obtain this knowledge. The relationships between structural data and melt even at the qualitative level, characteristics are less generally known.

### **1.6.3 Thermal properties**

An essential factor in product design is the expansion and contraction brought on by thermal energy. Glass expands as it is heated. There won't be any build-up of tension in the body if the temperature is uniform throughout the glass body and the body is not restrained. The different layers of glass will seek to expand differently if the body is not heated uniformly, which will lead to stress development in the glass. Thermal expansion has an impact on how much stress is created in this way. With very few exceptions, thermal expansion of glassware increases as temperature rises above 227-727°C. The network's capacity to absorb lattice expansion through the bending of bonds into empty structural interstices is thought to be the cause of the negative thermal expansion coefficients. The oxygen bridges are destroyed when alkali is added to the silica network, which causes the thermal expansion coefficient to increase monotonically [18]. When modifier ions are added to the glass network, bond bending and consequently the thermal expansion coefficient are prevented. Due to the two-dimensional nature of glass's structure and the poor connection between its dimensions, vitreous boric oxide exhibits a high thermal expansion coefficient. Borate anomaly is revealed by adding alkali oxides to the network of borate.

### **1.6.4 Mechanical properties**

Since glass is brittle, environmental variables, rather than the intrinsic strength of the connections composing the vitreous network, typically dictate how a glass will fracture. Glasses' fracture resistance varies depending on previous surface treatment, chemical environment, and natural tension, etc. The glasses are quite prone to breaking from temperature shock. Glasses have additional mechanical qualities that come naturally to the

substance. The network's structure and the specific boundaries in the material affect the elastic modulus. Strength of the bonds and atom packing density in the localised structure determine the hardness of glasses.

## **1.7 Glass Ceramics**

A twostep heat procedure result in crystallization. Nucleation is the first step, which occurs when the temperature exceeds to the  $T_g$ . The development of crystals at a higher temperature in the second step depends on composition. These steps can be carried out sequentially or concurrently.

### **1.7.1 Nucleation**

Nucleation is crucial because it regulates the process of total crystallisation. Classical nucleation theory is a theory that models the nucleation step. By modifying the classical nucleation hypothesis, Becker and Doring were responsible. Two premises form the basis of this theory:

- i) A sphere-shaped nucleus with a radius ( $r$ ) and a low surface energy.
- ii) Nuclei are regarded as macroscopic systems since they have identical chemical compositions and properties. Due to some discrepancies between the assumptions and results [18].

### **1.7.2 Growth**

The formation of nuclei depends upon many factors. Particularly, a crystal size of effective nuclei is required. Once the nuclei is formed the growth of these nuclei are started and formed the different shape of grain. The nuclei can be heterogeneous or homogenous in case of glass it is always heterogeneous. Since glass exhibit the multi comfort in the glass.

## **1.8 Properties of glass ceramics**

The properties of glass ceramics depends on many factors such as initial constituents, their amounts heat treatment temperature and heat treatment duration. The glass ceramics always

have better mechanical properties than their parent glass. Similarly, the thermal stability is also than the glass. Glass ceramics are superior to those of glass and ceramic. Glass-ceramic can have a variety of microstructures, including can alter the final product's qualities. This has an impact on the resultant glass-ceramic characteristics. Consequently, a variety of glass-ceramics can be created by combining parent glass and controlling the microstructure of crystalline phases [19].

## References

- [1] Jenkins, Francis A., Harvey E., Fundamentals of optics, Tata McGraw- hill Education, 1937.
- [2] J.E Shelby, introduction to Glass Science and Technology, 2<sup>nd</sup> Edition, The Royal Society of Chemistry, U.K. (2005).
- [3] J.W., Gibbs, Transaction of the Connecticut Academy of Arts and Science, 3, 1847-1878.
- [4] M. Volmer, Weber, A. Germ- formation in oversaturated figures, 119 (3/4) (1926) 277- 301.
- [5] L., Farkas, Z Phys Chem, (1927)125, 239.
- [6] R., Becker, Doring, Ann. Phys. 24, (1935) 719.
- [7] D.R., Cormier, L., Caurant, D., Montagne, L. nucleation, croissance applications (2013) 2571.
- [8] Al Saghir, Kholoud, Transparent ceramics by full crystallization from glass: application to strontium aluminosilicates, 2014.
- [9] S. Singh, K. Singh, J. Mol. Struct. 1081, (2015) 211-216.
- [10] S.K., Ts Jayasree, R., K, P.S.K., P, R.N., MukeshS, D. Bioceramics Development and Application Self Setting Bone Cement Formulations Based on Egg Shell Derived Tetracalcium Phosphate BioCeramics.5, (2005) – 6.
- [11] A., Zakery, Stephen Richard Elliot. Berlin: Springer, 135 (2007).
- [12] Jun, W. Klement, R.H. Willens, P.O.L. Duwez., Nature, 187(1960): 869.  
Telford, Mark, Material Today 7 (2004): 36.
- [13] Koroleva, O.N., L.A. Shabunina, V. N. Bykov, Glass and Ceramics 67.11 (2011): 340.
- [14] R.K. Mishra, V. Sudarsan, C.P. Kaushik, K. Raj, R.K. Vasta, M. Body, A.K. Tayagi, J. Non- Cryst. Solids 355(2009) 414.
- [15] Y. Shioya, Maeda, J. Electrochem. Soc.: Solid State Sci. Technol. 133(1986) 1943.

- [16] V.G. Plotnichenko, V.O. Sokolov, V.V. Kottashev, E.M. Dianov, J. Non – Cryst. Solids 306 (2002) 209.
- [17] T. Homma, R. Sato, Y. Benino, T. Komatsu, V. Dimitrov, J. Non - Cryst. Solids 272 (2000)1.
- [18] M.E.D.Mohamed, S.M. Saleem, I. Kashif, J. Mater. Sci.-Mater. Electron .10(1999)279.
- [19] S.K. Arya, S.S. Danewalia, K. Singh, J. Mater. Chem. C 4 (2016) 3328.

**Russelet al.**[1] investigated the nano-crystallization of  $\text{CaF}_2$  using  $\text{Na}_2\text{O}/\text{K}_2\text{O}/\text{CaO}/\text{CaF}_2/\text{Al}_2\text{O}_3/\text{SiO}_2$  glasses. Here, the increase of the  $\text{CaF}_2$  concentration leads to decrease in the glass transition temperature which further results in the  $\text{CaF}_2$  crystallization. The volume concentration of  $\text{CaF}_2$  crystalline increases with the thermal treatment temperature which further increases the viscosity near the crystallization of  $\text{CaF}_2$ . The crystal growth was found to be hindered due to a diffusional barrier was forming around each crystal.

**Kalampounias et al.** [2] studied the alkaline-earth silicate glasses produced by sol-gel were examined using infrared (IR) and Raman spectroscopy. The structure and vibrational modes of the sol-gel-prepared  $x\text{MO}(1-x)\text{SiO}_2$  ( $M = \text{Ca}, \text{Mg}$ ) binary silicate glasses have been studied using IR and Raman spectroscopies. Glasses with the following compositions were created:  $x = 0, 0-1, 0-2, 0-3, \text{ and } 0-4$ . The addition of alkaline earth metals oxides the  $T_g$  decreases and crystallisation temperature ( $T_c$ ) are also decreased. When compared to the identical glasses that were created using the traditional melting and quenching. The reported glass has better properties than conventional quenched glasses.

**Singhet al.** [3] studied about the melt and quench procedure was used to prepare the glass, which include four different transition element oxides. All of the examples are nanocrystalline glass ceramics, which naturally occur in a variety of nanocrystalline phases with varied roles played by the various transition metal oxides. As the molecular weight of the transition metal oxides in the glass composition increases, the density of the samples also increases.

**Jha et al.** [4] studied the influence of  $\text{SiO}_2\text{-K}_2\text{O-CaO-MgO}$  glasses' structural and optical properties on the field strength and electronegativity of  $\text{CaO}$  and  $\text{MgO}$ . The nature of these

glasses is amorphous. Higher MgO content glasses have a tendency toward phase separation. Some faint bands were seen in the FTIR spectra around 1393, 1461, and 1530  $\text{cm}^{-1}$ . These bands appear because CaO is more hydrophilic than MgO. Ca/Mg-O-H bonding is the cause of these bands. Mg's electronegativity and field strength result in the compactness of glasses with larger optical band gap of these glasses.

**Lahl** et al. [5] studied on the crystallisation kinetics of  $\text{AO-Al}_2\text{O}_3\text{-SiO}_2\text{-B}_2\text{O}_3$  glass, the effects of nucleating agents ( $\text{TiO}_2$ ,  $\text{ZrO}_2$ ,  $\text{Cr}_2\text{O}_3$ , and Ni), alkaline earth metals A (A = Ba, Ca, and Mg), and  $\text{Al}_2\text{O}_3$  were studied. Phase separation and a reduction in  $E_a$  are caused by an increase in the concentration of  $\text{Al}_2\text{O}_3$ . All findings are reviewed in relation to the chemical reactions and structural function of the Al ions as well as potential applications for the glasses. The Urbach energy enhanced with the modifier replacement.

**Kaur** et al. [6] studied influence of modifiers field strength on the lanthanum borosilicate glasses' optical, structural, and mechanical characteristics. All processed materials have had their Raman features investigated using Raman spectra, which is consistent with Fourier transform infrared (FTIR) spectroscopy. The substitution of alkaline earth metals in the decreasing field strength order (Mg > Ca > Sr > Ba) greatly affects the mechanical, structural, and optical characteristics of borosilicate glasses containing lanthanum. Since there are more of them, the optical band gap shrinks as a result of the replacement of heavy metals like barium in glass.

**Watts** et al. [7] studied about the examined glasses were created with a consistent network connection across the series and a systematic molar substitution of CaO for MgO. Glasses were created with a consistent network connection across the series and a systematic molar substitution of CaO for MgO. A single symmetric resonance with a chemical shift range of 8.2-12.7 parts per million (ppm) was visible in the  $^{31}\text{P}$  MAS NMR spectra, related to an

orthophosphate environment's presence. There was no proof that the bioactive glass had Si- O- P bonds downfield movement toward a species of the type sodium orthophosphate, was noticed when magnesium was substituted, indicating preferred sodium ions' relationship to the phosphate phase. The  $^{29}\text{Si}$  MAS NMR data showed that a prominent  $\text{Q}_2$  structure (79 ppm) was present, with a gradual change to a with increasing MgO substitution,  $\text{Q}_3$  structure (90 ppm). This research that suggests that magnesia acts more as an intermediate oxide.

**Rajyasree et al.** [8] studied the impact of modifier oxide (RO) on bismuth borate glass with increasing dopant concentration has been investigated by spectroscopic experiments. The addition of CuO in research using optical band gaps and FT-IR.  $\text{Ba}^{2+}$  ions successfully alter the network compared to  $\text{Ca}^{2+}$  ions. Intensities of optical absorption and photoluminescence indicate that the CuO addition. The current findings will therefore provide light on the structural analysis using IR-attenuated glasses that contain bismuth.

**Marzouik et al.** [9] studied about the optical and FTIR spectra of samples of binary bismuth silicate glass and samples having sections of  $\text{Bi}_2\text{O}_3$  substituted by SrO, BaO, or PbO were analysed to determine the optical properties and effects of gamma irradiation on bismuth silicate glasses containing SrO, BaO, or PbO. The strong UV near visible bands as well as the trace have both been found. Gamma radiation, bands, and a shift in the first UV band all had some effects on the signal's intensity, but no visible bands were produced. This conduct relates to the heavy metal oxide-containing glass ability to shield ( $\text{Bi}_2\text{O}_3$  content of 70%), the substituted oxide-containing samples (SrO, BaO, or PbO) exhibit certain differences. The type of oxide determines how it reacts to the gamma rays.

**Meng et al.** [10] by using the melt-quenching method, multicomponent glasses serving as slow-release fertilisers were created from the  $\text{SiO}_2\text{-P}_2\text{O}_5\text{-K}_2\text{O-MgO-CaO-CuO}$  system. The effects of CuO and  $\text{P}_2\text{O}_5$  addition on the structure of glasses were examined using FTIR,

Raman,  $^{31}\text{P}$ , and  $^{29}\text{Si}$  MAS NMR spectroscopies. The study showed that in the structure of glass, the  $\text{Cu}^{2+}$  ions prefer to connect with the phosphorus  $\text{Q}^1$  species, producing the  $\text{Q}^0$  species with chemically stable P-O-Cu bonds while dislodging the  $\text{Ca}^{2+}$  and  $\text{Mg}^{2+}$  ions.

**Gajek** et al. [11]  $\text{MgO-CaO-Al}_2\text{O}_3\text{-SiO}_2\text{-K}_2\text{O-(BaO)}$  glass were studied and reported the effects on the structure and microstructure of fast burnt glazes were investigated in this work. Studies using FTIR and Raman spectroscopy have demonstrated that the network of all glasses was depolymerized by barium ions (modifier ions). The energy barrier for crystallisation was lowered in this manner.

**Jha** et al. [12] studied about the because  $\text{MgO}$  serves as a network former, its replacement of  $\text{CaO}$  in the current glasses boosts their endurance. The micro-hardness ranges from 464-502 Hv, similar to the hardness of bone is observed. Even after soaking in simulated body fluid (SBF) solution, none of the glasses have any crystalline peaks. On the other hand, when glasses are wet, Urbach energy diminishes.  $\text{MgO}$  substitution for  $\text{CaO}$  decrease the bioactivity of these glasses.

**Lesniak** et al. [13] has reported the link between the phase composition and opacity of glass-ceramic glazes made from the  $\text{SiO}_2\text{-Al}_2\text{O}_3\text{-MgO-K}_2\text{O-Na}_2\text{O}$  system using a varied molar ratio of  $\text{SiO}_2/\text{Al}_2\text{O}_3$ . The phase composition derived from the glazes was identified using X-ray diffraction (XRD). A high molar ratio of the oxides  $\text{SiO}_2$  to  $\text{Al}_2\text{O}_3$  promotes the crystallisation of forsterite and enstatite, according to the results of the tests (XRD and Raman).

**Partyka** et al. [14] examined the internal aluminium-silicon-oxide lattice of glass and ceramic materials. To ascertain the true composition of the samples that were obtained, a chemical analysis was performed. After the heat-treatment process of the  $\text{SiO}_2\text{-Al}_2\text{O}_3\text{-Na}_2\text{O-K}_2\text{O-CaO}$  system is affected by the molar ratio of  $\text{SiO}_2/\text{Al}_2\text{O}_3$ , pseudo wollastonite, anorthite, and the

vitreous phase are discovered. For the inner structural study, X-ray diffraction (XRD), Raman spectroscopy, as well as FTIR spectroscopy, were employed.

**Mahdy** et al. [15] studied about the system of glasses made up of CaO, MgO, SiO<sub>2</sub>, and CaF<sub>2</sub> was examined. Na<sub>2</sub>O and P<sub>2</sub>O<sub>5</sub>, respectively, were added to modify the concentrations of MgO and SiO<sub>2</sub> in a methodical manner. The creation of the glasses involved a conventional melting procedure. An XRD study showed that the generated glass was amorphous. More Na<sub>2</sub>O and P<sub>2</sub>O<sub>5</sub> were added, and as a result of the changed structure, the observed values of  $\rho$  and  $V_m$  increased, respectively, from 2.76 to 2.86 g/cm<sup>3</sup> and from 20.06 to 20.60 cm<sup>3</sup>/mol.

**Szumer** et al. [16] studied the effect of MoO<sub>3</sub> on the silicate-phosphate glasses. According to the results, molybdenum ions in the examined glasses function as modifiers, which are supported by Raman spectroscopic examinations. The observed results imply that two separate chemical environments that affect phosphorus atoms are present as a result of the introduction of molybdenum ions into the glass structure under study. It is determined that an increase in MoO<sub>3</sub> content weakens the structure of system glasses and causes the degree of silicate-phosphate framework depolymerization to gradually increase.

According to the Cole-Cole representation and Raman spectroscopic data studied by **Rim** et al. [17], the disorder of the glass matrix is dramatically reduced with growing non-bridging oxygens per tetrahedra (NBO/T) and lowering dispersion of the inter-ionic Coulomb interaction. Alkaline-earth metals' ionic radii expand in ATSO glasses as the pathway's dimension contracts. Therefore, the distinct bands from either the Ti-bearing complex or the Si-bearing complex increase the randomness of the NBO/T distribution and the unpredictability of the system.

**Muniz** et al. [18] studied the network structure using XRD and Raman spectroscopy. Moreover, similar Eu<sub>2</sub>O<sub>3</sub>-doped samples employed Eu<sup>3+</sup> as a local structural probe. They were

able to look into the local environment of precursor glass and glass-ceramic due to the luminescence characteristics (emission spectra and transition durations). With 20 nm-sized crystals, calcium fluoride nanostructured glass-ceramic was produced with high transparency (between 60 and 70 percent in the visible region). The synthetic materials' refractive indices glasses, which is necessary for excellent transmittance, was too near to that of precepted crystals. The duration of the matrix-embedded  $\text{Eu}^{3+}$  ions have demonstrated that the glass-ceramic environment has reduced phonon energy. This matrix is a superior choice for photonics applications than in glass as-made.

**Wang et al. [19]**In this study, the mixed alkaline earthoxynitride glasses of (Ca, Mg) - Si - Al - O - N have been successfully pre-pared via the sol-gel method. There is an obvious mixed alkaline eartheffect existed in the dynamic performances of thermal expansion coefficient and glass transition temperature ( $T_g$ ), which exhibits the minimum value in the  $\text{CaO}/(\text{CaO} + \text{MgO})$  molar ratio of 0.25 and 0.75respectively.In addition, the oxynitride glasses' molar volume and density rise when CaO replaces MgO, while their Vickers hardness and compressive strength decreases.

**Zhang et al. [20]** studied about the structure and properties of glass ceramics are altered as a result of the nucleating agent's impact on the amorphous phase. Raman spectroscopy is utilised during the progression from glass to glass-ceramics with various  $\text{Cr}_2\text{O}_3$ doping. Forthe amorphous and crystalline phases of precursor glass, nucleating glass, and glass-ceramics, respectively, the Raman spectra were examined. Raman spectra showed the stretching and bending vibrations of the glass network. Data from the fitting peak showed that the glass network was depolymerizing and the bridge oxygen link had broken.

The  $\text{CaO-Al}_2\text{O}_3\text{-MgO-SiO}_2$  (CAMS) slag glass-ceramics are studied using a viscometer, differential scanning calorimetry (DSC), X-ray diffraction (XRD), scanning electron

microscopy (SEM), Raman spectroscopy by **Denget al.**[21].Physicochemical properties to determine the exact effect of  $\text{CaF}_2$  on the viscosity, structure, and performance of the glass-ceramics. The findings demonstrate that low  $\text{CaF}_2$  concentrations promote silicate network depolymerization, which lowers the melting point, viscosity, and viscous activation energy of glass.

**Ariane** et al. [22] studied about the composition, microstructure, thermal and mechanical properties, and impact of  $\text{P}_2\text{O}_5$  and  $\text{Al}_2\text{O}_3$  on glasses and glass-ceramics in the **LMAS** system. Study has been done on additives. The glass and glass-ceramic transition temperature increase with the  $\text{P}_2\text{O}_5$  and  $\text{Al}_2\text{O}_3$  content, whereas melt viscosity decreases at high temperatures. Raman, and FT-IR spectroscopies have demonstrated the production of a glass phase rich in silica that serves as a matrix for crystallites that contain  $\text{Al}_2\text{O}_3$  and  $\text{P}_2\text{O}_5$ . The concentration of  $\text{Al}_2\text{O}_3$  affects the crystallites form and aspect ratio.

## **2. Motivation and objective**

Based on the literature survey of glasses, it is found that the crystallisation behaviour of  $55\text{SiO}_2$ - $10\text{K}_2\text{O}$ - $(35-x)\text{CaO}$ - $x\text{MgO}$  ( $x= 0, 5, 10, 15, 20, 25,$  and  $35$  mol%) glasses are rarely reported. So, the objectives of the present work are as follows:

1. As prepared glasses will be converted into glass-ceramics.
2. Glass ceramics will be characterized for their optical and structural properties to access the impact of formed crystalline phases.

## References

- [1] C. Russel. Nanocrystallization of  $\text{CaF}_2$  from  $\text{Na}_2\text{O}/\text{K}_2\text{O}/\text{CaO}/\text{CaF}_2/\text{Al}_2\text{O}_3/\text{SiO}_2$  Glasses. *Chem. Mater.* 17 (2005) 5843- 47.
- [2] A.G. K Salampounias. IR and Raman spectroscopic studies of sol–gel derived alkaline-earth silicate glasses. *Bull. Mater. Sci.* 34 (2) (2011) 299–303.
- [3] S.Singh, K. Singh. Nanocrystalline glass ceramics: Structural, physical and optical properties. *J. Mol. Struct.* 34 (2) (2014) 299-303.
- [4] P. Jha. Effect of Field Strength and Electronegativity of CaO and MgO on Structural and Optical Properties of  $\text{SiO}_2\text{–K}_2\text{O}\text{–CaO}\text{–MgO}$ . *Glasses Silicon.* 8 (2016) 437–442.
- [5] N. Lahl. Crystallisation kinetics in  $\text{AO}\text{–Al}_2\text{O}_3\text{–SiO}_2\text{–B}_2\text{O}_3$  glasses (A = Ba, Ca, Mg) *J. Mater. Sci.* 35 (2000) 3089 - 96.
- [6] G. Kaur. Effect of modifiers field strength on optical, structural and mechanical properties of lanthanum borosilicate glasses, *J Non Cryst Solids* 358 (2012) 2589 - 96.
- [7] S.J. Watts. Influence of magnesia on the structure and properties of bioactive glasses. *J Non Cryst Solids.* 356 (2010) 517–524.
- [8] Ch. Rajyasree, D. Krishna Rao. Spectroscopic investigations on alkali earth bismuth borate glasses doped with CuO. *J Non Cryst Solids.* 357. (3) (1)(2011) 836-841.
- [9] M. A. Marzouk · H. A. ElBatal · F. M. EzzElDin. Optical Properties and Effect of Gamma Irradiation on Bismuth Silicate Glasses Containing SrO, BaO or PbO. *Silicon* 5 (2013) 283–295.
- [10] Meng, Yong. In situ high temperature X-ray diffraction study on high strength aluminous porcelain insulator with the  $\text{Al}_2\text{O}_3\text{SiO}_2\text{–K}_2\text{O}\text{–Na}_2\text{O}$  system. *Appl. Clay Sci* 132 (2016) 760-767.
- [11] Gajek, Marcin. The crystallization and structure features of glass within the  $\text{K}_2\text{O}\text{–MgO}\text{–CaO}\text{–Al}_2\text{O}_3\text{–SiO}_2\text{-(BaO)}$  system. *J.Mol. Struct* 1220 (2020) 128747.
- [12] P. Jha, K. Singh. Effect of MgO on bioactivity, hardness, structural and optical properties of  $\text{SiO}_2\text{–K}_2\text{O}\text{–CaO}\text{–MgO}$  glasses. *Ceram. Int* 42.1 (2016) 436-444.

- [13] M. Lesniak, J. Partyka, K. Pasiut, M. Sitarz. Microstructure study of opaque glazes from  $\text{SiO}_2\text{-Al}_2\text{O}_3\text{-MgO-K}_2\text{O-Na}_2\text{O}$  system by variable molar ratio of  $\text{SiO}_2/\text{Al}_2\text{O}_3$  by FTIR and Raman spectroscopy. *J. Mol. Struct* (2016) 1-11.
- [14] J. Partyka, M. Lesniak. Raman and infrared spectroscopy study on structure and microstructure of glass–ceramic materials from  $\text{SiO}_2\text{-Al}_2\text{O}_3\text{-Na}_2\text{O-K}_2\text{O-CaO}$  system modified by variable molar ratio of  $\text{SiO}_2/\text{Al}_2\text{O}_3$ . *Spectrochimica Acta Part A: Molecular and Biomolecular Spectroscopy* 152 (2016) 82–91. *Spectrochimica Acta Part A: Spectrochim. Acta A Mol. Biomol. Spectrosc.* 152 (2016) 82–91.
- [15] Ebrahim A. Mahdy, Z.Y. Khattari b, Waheed M. Salem c, S. Ibrahim. Study the structural, physical, and optical properties of  $\text{CaO-MgO-SiO}_2\text{-CaF}_2$  bioactive glasses with  $\text{Na}_2\text{O}$  and  $\text{P}_2\text{O}_5$  dopants *Mater. Chem. Phys* 286 (2022) 126231.
- [16] Szumera, Magdalena. Structural investigations of silicate–phosphate glasses containing  $\text{MoO}_3$  by FTIR, Raman and  $^{31}\text{P}$  MAS NMR spectroscopies. *Spectrochimica Acta Part A: Spectrochim. Acta A Mol. Biomol. Spectrosc.* 130 (2014)1-6.
- [17] Rim, Young Hoon..Influence of ionic radius of alkaline-earth metals in ion conducting 2 (Ca, Sr, Ba)  $\text{O}_2\text{TiO}_2\text{SiO}_2$  glasses. *J. Non Cryst Solids* 500 (2018)336-344.
- [18] R. F. Muniz. Thermal, optical and structural properties of relatively depolymerized sodium calcium silicate glass and glass-ceramic containing  $\text{CaF}_2$ . *Ceram. Int.* 47.17 (2021)24966-24972.
- [19] Wang, Huili. The influence of the mixed alkaline earth effect on the structure and properties of (Ca, Mg)–Si–Al–O–N glasses. *Ceram Int.* 47.9 (2021)12276-12283.
- [20] Zhang, YuXuan. Raman spectroscopic study of irregular network in the process of glass conversion to  $\text{CaO-MgO-Al}_2\text{O}_3\text{-SiO}_2$  glass-ceramics. *J. Non Cryst Solids* 563 (2021)120701.
- [21] Deng, Leibo. Effect of  $\text{CaF}_2$  on viscosity, structure and properties of  $\text{CaO-Al}_2\text{O}_3\text{-MgO-SiO}_2$  slag glass ceramics *J. Non Cryst Solids* 500 (2018) 310-316.
- [22] Ariane, Khalissa. Effect of  $\text{P}_2\text{O}_5$  and  $\text{Al}_2\text{O}_3$  on crystallization, structure, microstructure and properties of  $\text{Li}_2\text{O-MgO-Al}_2\text{O}_3\text{-SiO}_2\text{-TiO}_2\text{-ZrO}_2$  glass ceramics. *Bol SocEspCeram*(2020).

All the samples were synthesized using the melt quench method followed by controlled heat treatments. Different experimental techniques were used to characterise glass ceramics. This chapter includes the technical details of techniques.

### 3.1 Sample preparation

#### 3.1.1 Preparation of glasses

Glasses with a composition of  $55\text{SiO}_2\text{-}10\text{K}_2\text{O}\text{-(}35\text{-x)CaO-xMgO}$  ( $x = 0, 5, 10, 15, 20, 25,$  and  $35$  mol%) were formed. Starting materials were used without further purification because they were 99 percent pure. All chemical were used in their oxide form except  $\text{K}_2\text{CO}_3$  (potassium carbonate) was measured using the gravimetric factor of 1.47. The initial stoichiometric constituents were grounded in an agate mortar and pestle in acetone medium for 2 hours (h) [1]. These ground powders were transferred into  $\text{Al}_2\text{O}_3$  crucible and melted in electric furnace on a high temperature programmable  $1550^\circ\text{C}$ . The glass composition are given in table 3.1.

**Table 3.1** Glass labels along with their composition in mol%

Sample label	$\text{SiO}_2$	$\text{K}_2\text{O}$	$\text{CaO}$	$\text{MgO}$
CM-0	55	10	35	0
CM-10	55	10	25	10
CM-20	55	10	15	20
CM-30	55	10	5	30

The furnace was kept at intermediate temperatures ( $300, 600, 900,$  and  $1200^\circ\text{C}$ ) for 0.5 hours to increase the chemical mixtures' ability to fuse together. To homogenize the melt, it was also kept at  $1550^\circ\text{C}$  for an hour. The melt was quenched on a foundation made of a thick copper

plate in the air to produce the glass flakes. The other details of sample were given in our earlier publication [2-4].

### **3.1.2 Preparation of glass-ceramic pellets**

By applying a hydraulic pressure of 1.25 kN/m<sup>2</sup> for 10 seconds were applied to the fine and ground powders of the as-quenched samples to form the pellets with a diameter of 5 mm and a thickness of 2–3 mm. The nucleation/growth temperature of 850 °C was chosen for the controlled heat treatment of all the glasses based on DTA. The samples were heated in the furnace for 1 hour and 10 hours before it cooled to room temperature to convert them into glass ceramics. Some of the crystalline phase embedded in the glass matrix tends to crystallize as a result of the controlled heat treatment. The heat-treated glass samples were given new labels depending on the time they were heated in the furnace. CM0(1), CM10(1), CM20(1), CM30(1) are the labels for glass-ceramics that were heated in the furnace for 1 hour at 850°C. Similarly, CM0(10), CM10(10), CM20(10) and CM30(10) are the labels for glass-ceramics that were heated in furnace for 10 hours at 850°C [5].

### **3.2 Characterizations of as quenched/heat-treated samples**

As explained in this and the next sections, all of the glass samples have been identified using different methods. The glass preparation and their characterization are given in the flow chart (figure 3.1)

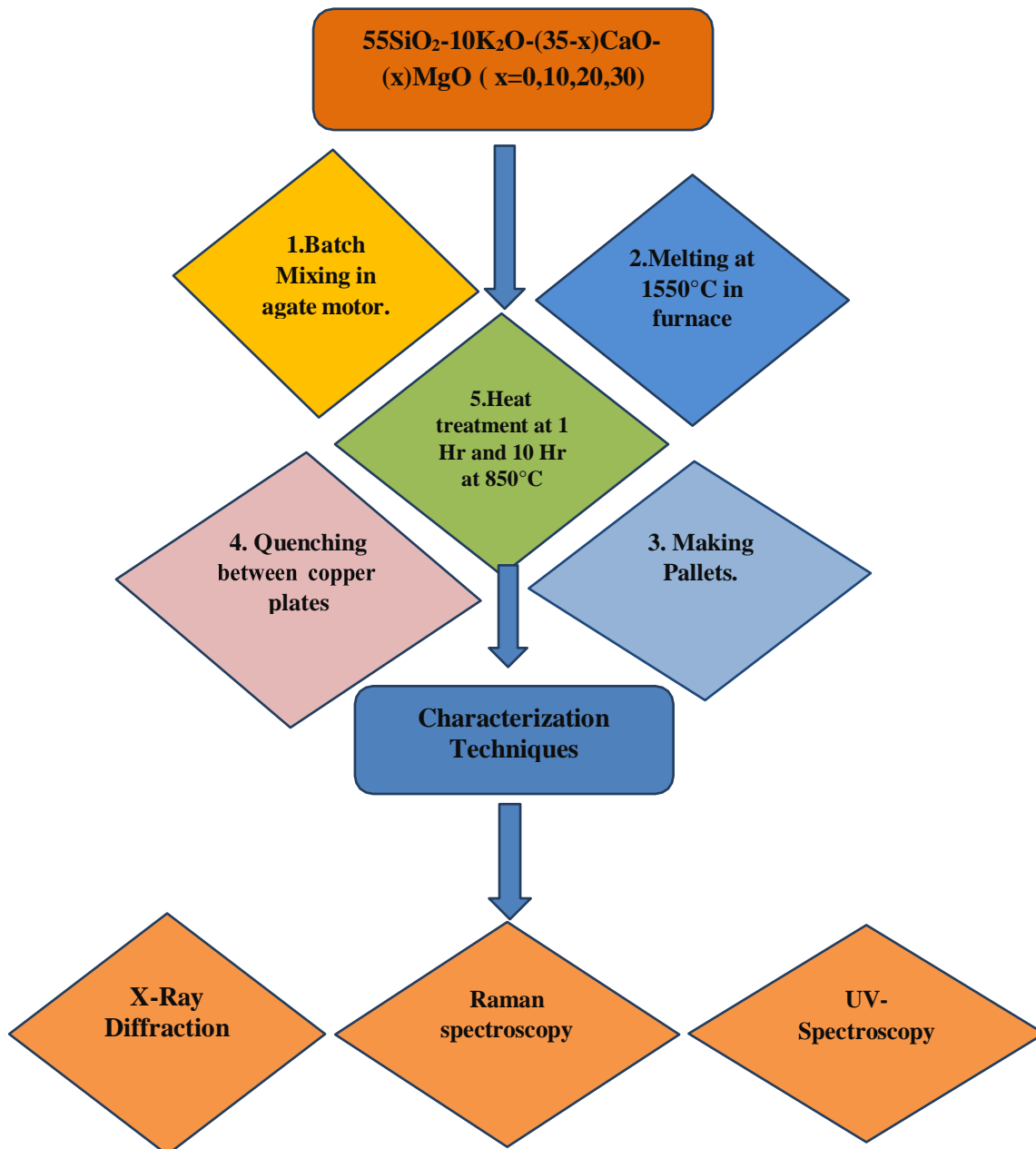


**Figure 3.1** Experimental steps followed in order to study the properties of the given heat-treated glasses

### 3.2.1 X-ray diffraction (XRD)

The X – ray diffraction was used to know the nature and phase formation in glasses and glass ceramics, respectively. The X-rays diffraction patterns were produced by cathode ray tubes are collimated to concentrate them and directed onto the sample after being filtered to produce monochromatic radiation [6]. The monochromatic X-rays that are constructively interfered with and diffracted from the crystalline sample are the basis of X-ray diffractometry (XRD). The interaction between sample incoming photons leads in constructive interference of the

diffracted rays when the Bragg's law condition ( $2d \sin\Theta = n\lambda$ ) is satisfied. The crystal's interplanar spacing ( $d$ ) and the wavelength of X-rays, which ranges from 0.1 to 100, are exactly the same. In light of this, Bragg's rule predicts that the X-ray and crystal interactions would result in the diffraction patterns shown in Figure 4.1. XRD patterns can be used to calculate the structure specifications including the volume of crystalline phases, crystallite size and strain. Amorphous materials like glass lack diffraction peaks. Instead of diffraction peaks one or more broad halos are shown in glasses. The glass composition gets affected where the broad halos are located. The presence of many broad halo patterns in the XRD patterns of glasses shows a clear indication of phase separation. The compositions with immiscible phases in the melt result in the phase separated glasses. The general decrease of energy controls the phase separation event. When the mixture of two components is separated, the free energy is reduced, and glass becomes phase separated. In other cases, homogeneous melt without any phase separation results in a lowering of free energy [7].

Glass-ceramics XRD patterns give sufficient details regarding the crystalline phases. Crystalline peaks can be found in the basic glass matrix of glass-ceramics. In samples of the crystalline phases, it is possible to identify the volume fraction of different phases, crystallite size, and kind of strain, such as compressive and tensile. Using Rigaku Smart lab SE powder X-ray diffractometer and Cu-K $\alpha$  monochromatic radiation ( $\lambda = 1.54 \text{ \AA}$ ), the XRD patterns of the as-quenched samples were captured for this work. Measurements were made between the  $2\Theta$  ranges of  $10^\circ$  and  $90^\circ$  in the air. The step size was preserved at  $0.017^\circ$  and the scanning speed was fixed at  $3^\circ/\text{min}$ . The JCPDS cards were used with high scorer software to match the crystalline phases and peak positions [8].

### **3.2.2 Raman spectroscopy**

Raman spectroscopy is a supplementary method for calculating information about the structural units of the glasses. This method could be used to understand some of the broad

band silica that FTIR spectra were unable to resolve well. This method is sensitive for the wave number where FTIR is insensitive. While FTIR spectroscopy focuses on changes in the dipole moment, Raman spectroscopy focuses on changes in a molecule's polarizability. On a Renishaw in through Raman spectrometer, the spectra of a representative powdered glass are traced within the range of 50-1200  $\text{cm}^{-1}$ . The observations are conducted using a 20 mW. Argon (Ar) laser at 514.5 nm. Silicon is utilised as a standard to calibrate the device at 520  $\text{cm}^{-1}$ . The instrument's spectral resolution is 1  $\text{cm}^{-1}$  [9-11].

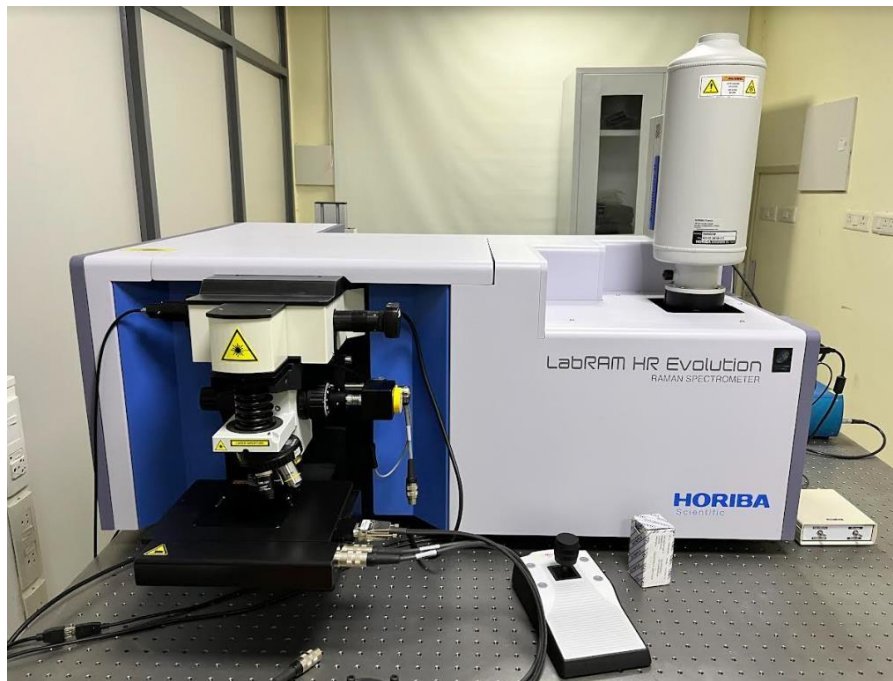


**Figure 3.3 Raman Spectroscopy Instrument**

### **3.2.3 UV-visible spectroscopy**

The relationship between optical band gap energy ( $E_g$ ) and absorption coefficient ( $\alpha$ ) for tiny values of absorption coefficients ( $\alpha \leq 10^{-4}$ ) is presented when incident UV-Visible light is transmitted through material that has been dissolved in the appropriate solvent [12].

$$\alpha h\nu = B(h\nu - E_g)^n \quad (3.1)$$

In this case,  $h\nu$  stands for the energy photon.  $n$  can have a variety of numbers, such as 2, 3, and 1/2 for direct transitions that are allowed and disallowed respectively.  $B$  is a constant also referred to as the band tailing parameter.

When the energy of the incident photons rises, the absorbance coefficient of the materials exhibits an exponential increase. Following is a comparison of the absorption coefficients in the Urbach tail region.

$$\alpha = \alpha_0 \exp(h\nu / E_U) \quad (3.2)$$

where,  $\alpha_0$  and  $E_U$  are the constant and the Urbach energy [7]. By using the inverse of the slope of the linear portion of the curve between  $\ln$  and  $h\nu$ , the Urbach energy of the glasses may be computed [13]. All samples' optical characteristics can also be obtained in powder form. The Kubelka-Munk function is presented for controlling optical band gap and different parameters as follows:

$$F(R) = \frac{\alpha}{s} = \frac{1-R^2}{2R} \quad (3.3)$$

where, respectively,  $R$  and  $s$  stand for reflectance and scattering constants. All samples UV-visible spectra were captured between the wavelengths of 200 nm and 800 nm using a double beam spectrophotometer (HITACHI U-3900 H). The resolution is 0.20 nm, and the dispersed speed is 120 nm min<sup>-1</sup>. The powder sample spectra are captured in reflectance mode [14-16].

## References

- [1]. B.D. Cullity, Elements of X-Ray Diffraction, Addison-Wesley Publishing Company Inc.(1956).
- [2]. Y.-M. Sung, S.A. Dunn, J.A. Koutsky, J. Eur. Ceram. Soc. 14 (1994) 455.
- [3]. J.E. Shelby, Introduction to Glass Science and Technology, 2<sup>nd</sup>edn, The Royal Society of Chemistry, Cambridge-UK(2005).
- [4]. W. Smykatz-kioss, Differential Thermal analysis application and results in mineralogy, springer-verlag Berlin, Heidelberg (1974).
- [5]. B. Schrader (ed.), Infrared and Raman Spectroscopy: Methods and applications, VCH Publishers, Inc., New York (1995).
- [6]. V.Raghvan, Materials Science and Engineering (5<sup>th</sup> Edition) Prentice-Hall of India Pvt.Ltd.(2004).
- [7]. F. Urbach, Phys. Rev. 92 (1953)1324.
- [8]. T.Kokubo, H.Kushitani, S.Sakka, T.Kitsugi, T.Yamamuro, J.Biomed.Mater.Res.24 (1990) 721.
- [9]. D. Zhang, M. Hupa, H.T. Aro, L. Hupa, Mater. Chem. Phys. 111 (2008) 497.
- [10]. P. Siriphannon, Y. Kameshima, A. Yasumori, K. Okada, S. Hayashi, J. Biomed. Mater. Res. 60 (2002) 175.
- [11]. S. Singh, Structural and Bioactive Properties of Fe/Mn Oxides substituted Sodium Silicate Glasses, Ph.D Thesis (2017) Thapar University, Patiala.
- [12]. P. Siriphannon, Y. Kameshima, A. Yasumori, K. Okada, S. Hayashi, J. Biomed. Res. 60 (2002) 175.
- [13]. Mohini G.Jagan, Baskaran G Sahaya, Kumar V Ravi, M Piasecki, N Veeraiah, Mat. Sci & Eng C 57 (2015) 240
- [14]. Ch.Vijaya Kumari, P.Sobhanachalam, C.K Jayasankar, N.Veeraih, V.Ravi Kumar, ceram.Int. 43(2017)4335
- [15]. K. Shimizu, T. Mitani, New Horizons of Applied Scanning Electron Microscopy, Springer Berlin Heidelberg, Germany (2010).
- [16]. Indian Pharmacopopia (IP), Vol-1, 7th edition, Indian Pharmacopopia commission, Ghaziabad (2014).

## 4.1 X-Ray diffraction

The XRD patterns of all the heat treated glasses are shown in figure 4.1.

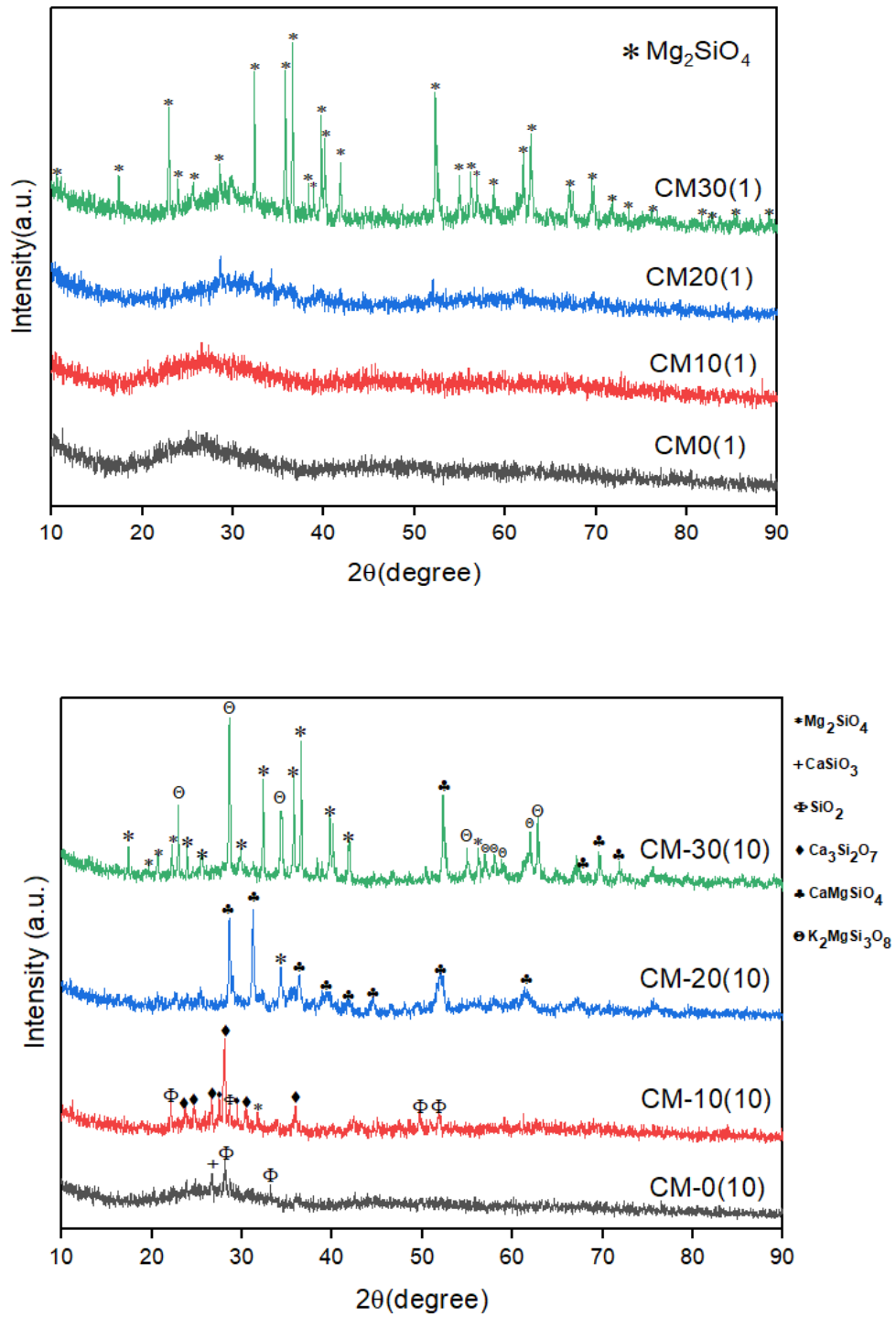


Figure 4.1 XRD pattern of (a) 1 hour heat treated CM series, (b) 10hour heat treated CMseries

The CM0 (1), CM10 (1) are completely amorphous after 1 hour (h) heat treatment of glasses. As MgO content increases in the glasses, CM20 (1) is started to crystallize some vary XRD peaks are observed as seen in figure 4.1(a). In contrast to these glasses, CM30 (1) glass exhibit  $Mg_2SiO_4$  phase. As the heat treatment duration increases from 1h to 10h, all the glass converted into glass ceramics as observed in figure 4.1(b). The CaO containing glass exhibit mainly  $SiO_2$  crystalline phase CM0 (10)). As MgO increases, the crystallization tendency in the glasses are increased. The crystalline phases and JCPD card number along with their labels are given in table 4.1. As heat treatment duration (10h) and MgO content increases instead of CaO the volume fraction of crystalline phases are also increases, and different crystalline phases are evolved. Interestingly, the MgO content increases the crystallization tendency in glasses and prevent the formation of  $SiO_2$  as seen in table 4.1[1].

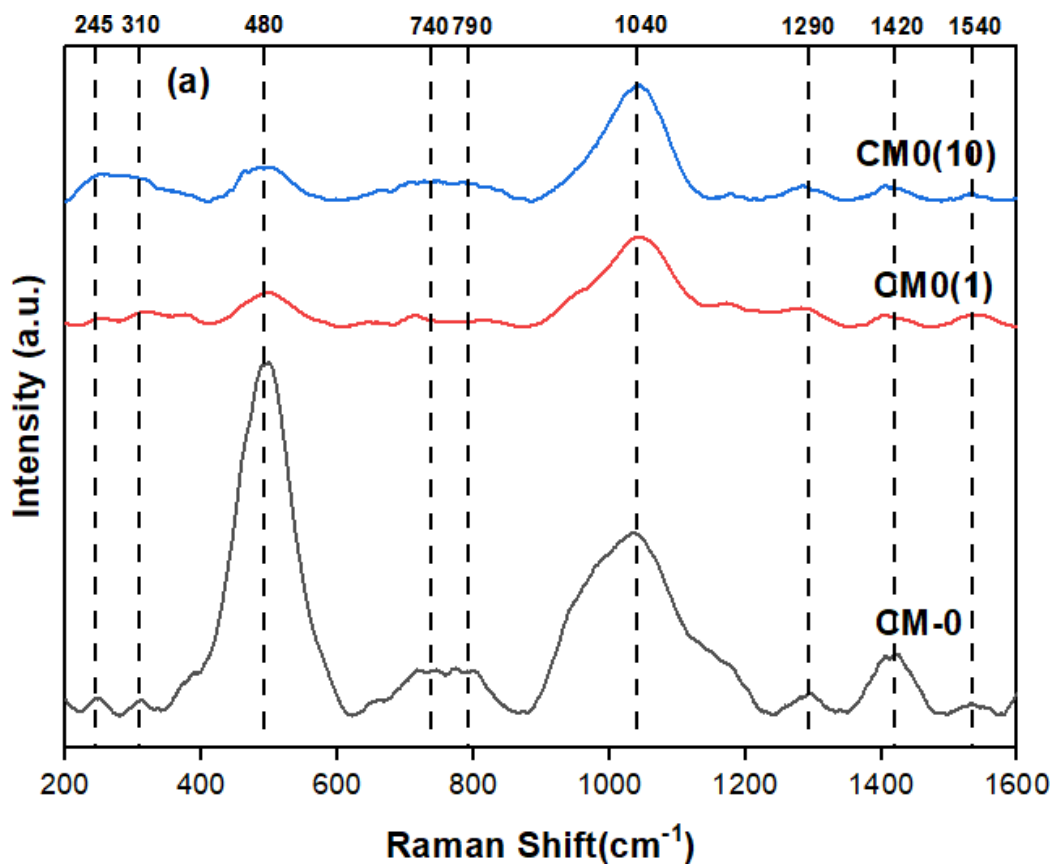
Table 4.1 Crystalline Phases and their volume Fraction formed in present glass- ceramics

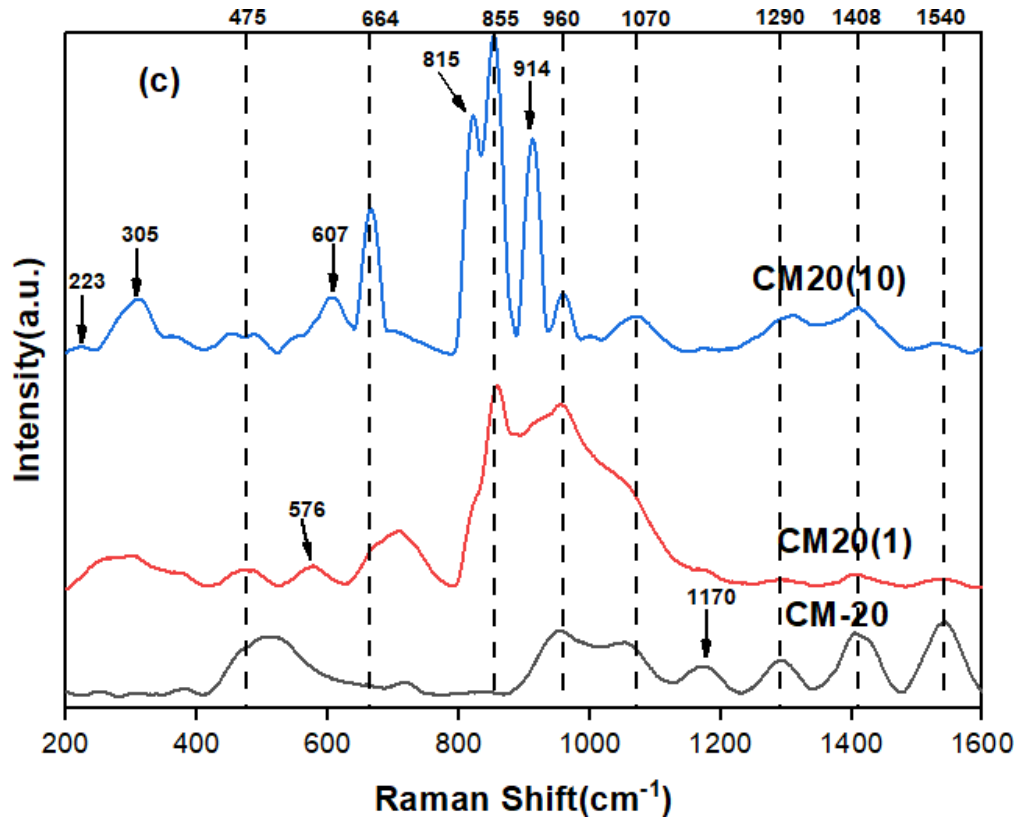
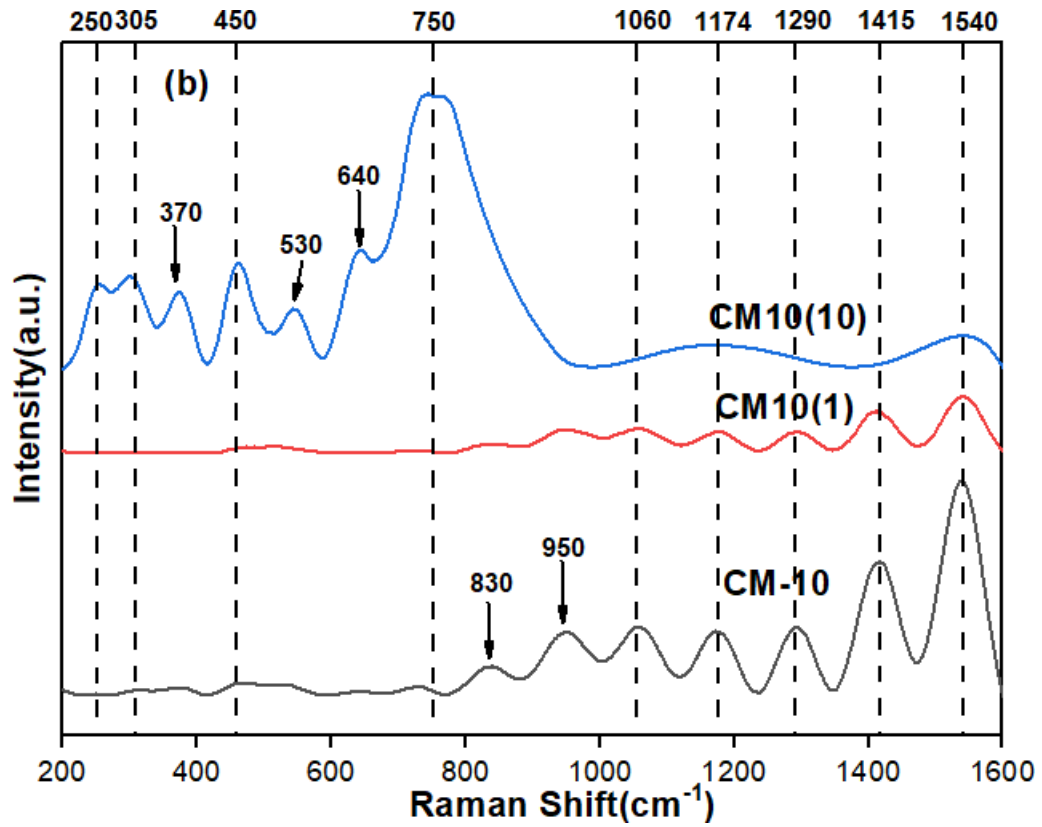
<b>Sample id (Time hr)</b>	<b>Crystalline Phases</b>	<b>Nature</b>
CM0(1)	-	Glass
CM10(1)	-	Glass
CM20(1)	-	Glass-Ceramic(Partial)
CM30 (1)	$Mg_2SiO_4(00-021-1260)$	Glass-Ceramic
CM0 (10)	$SiO_2(01-081-1665)$ (00-04601242) $CaSiO_3(01-075-1092)$	Glass-Ceramic
CM10 (10)	$SiO_2(01-081-1665)$ (00-04601242) $Mg_2SiO_4$ (00-021-1260) $Ca_3Si_2O_7(01-075-1092)$	Glass-Ceramic
CM20 (10)	$Mg_2SiO_4(00-021-1260)$ $CaMgSiO_4$ (01-075-1092)	Glass-Ceramic
CM30 (10)	$Mg_2SiO_4$ (00-021-1260)	Glass-Ceramic

	CaMgSiO <sub>4</sub> (01-075-1092)	
	K <sub>2</sub> MgSiO <sub>4</sub> (00-019-0973)	

According to research in silicate glasses it is reported that the initial nucleation of a phase rich in silica is followed by the inclusion of additional ions during the crystallization of silicate glasses [2].

#### 4.2 Raman spectra analysis





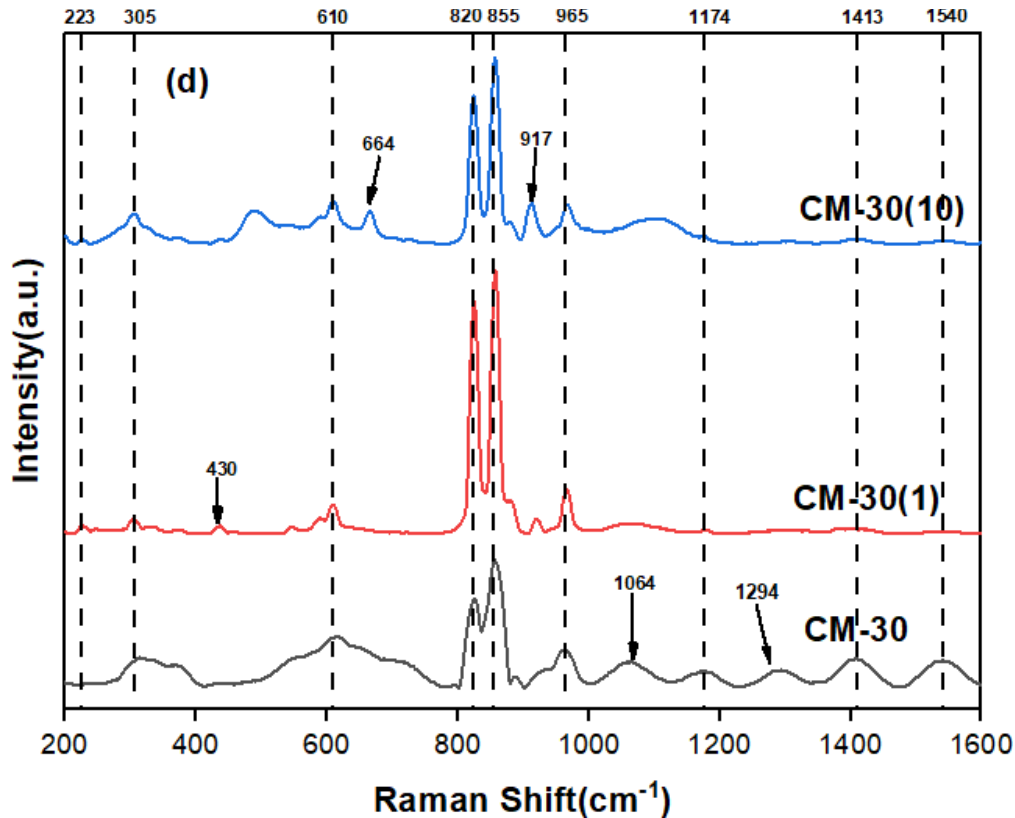
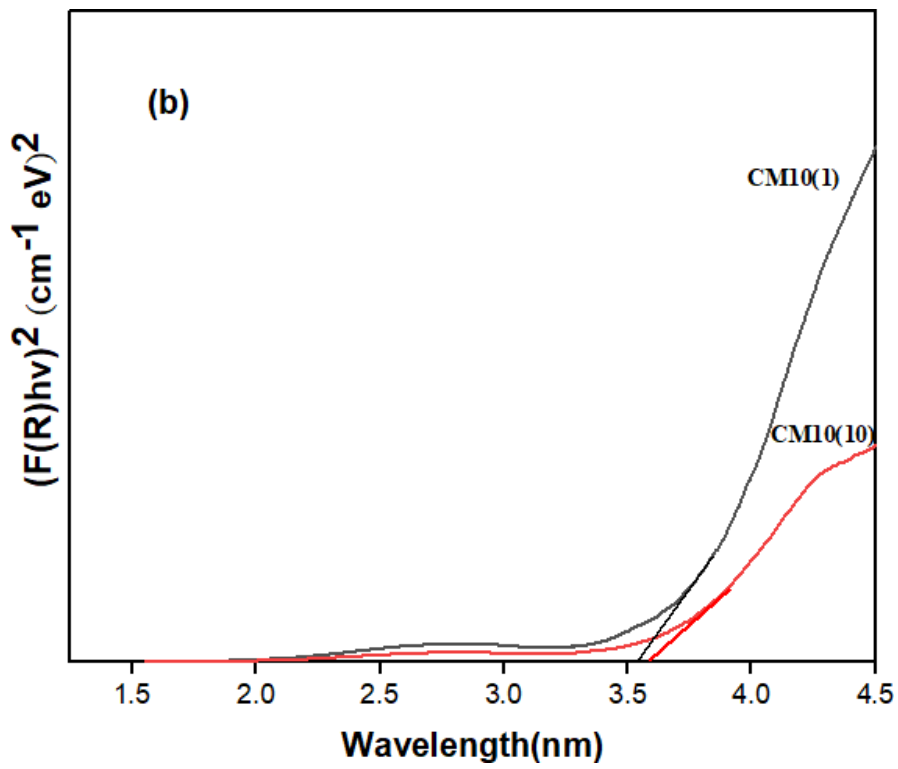
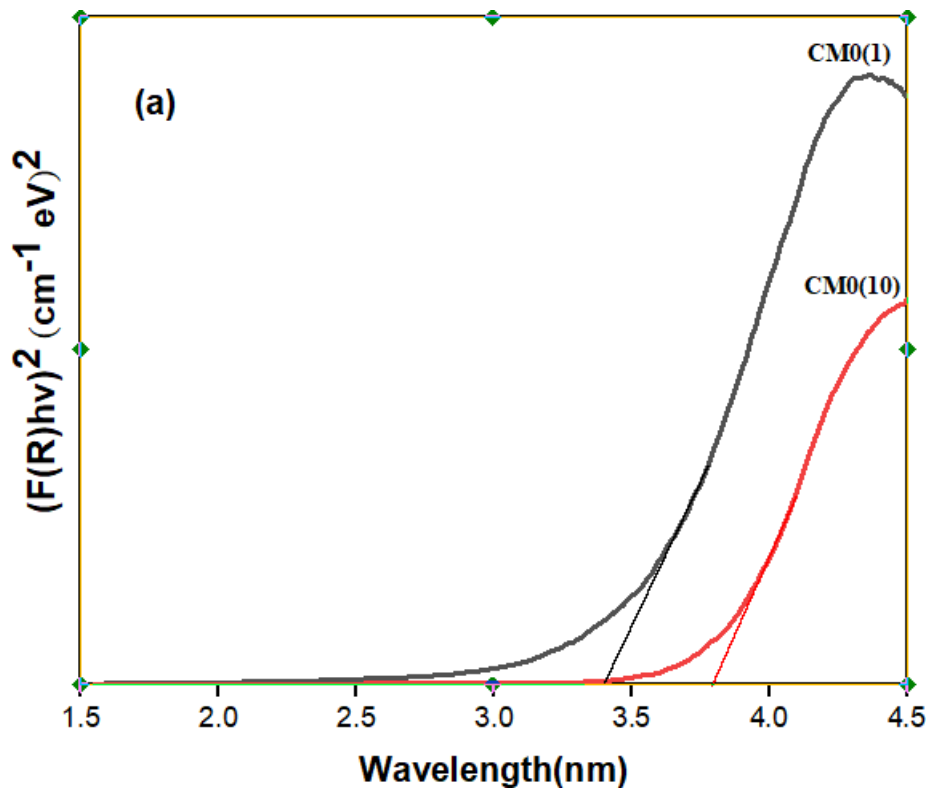


Figure 4.2 Raman spectra of (a)CM0, CM0(1) and CM0(10), (b) CM10, CM10(1) and CM10(10), (c) CM20, CM20(1) AND CM20(10) and (d) CM30, CM30(1) and CM30(10)

Figure 4.2 shows the Raman spectra of the current glasses. Throughout the measured wave number range, wide Raman bands in the region of 800-1200  $\text{cm}^{-1}$  are seen in all the glasses. More than one closely spaced Raman bands overlapping causes a broad band to appear in the spectra. According to reports, some  $Q_i$  units-mostly  $Q_2$ -contribute to spectra with many bands. As a result, it is more challenging to interpret the spectra [3–4]. With regard to various Si-O vibrations, Raman bands over 800-1200  $\text{cm}^{-1}$  are relevant. The depolymerized units' bending vibrations are represented by the Raman bands at 600  $\text{cm}^{-1}$  [5]. Bridging oxygen atoms between silica tetrahedra cause symmetric stretching vibrations that cause Raman bands to appear at 700-850  $\text{cm}^{-1}$ . This spectrum comprises vibrations of the orthosilicate units at 790, 807, and 850  $\text{cm}^{-1}$ , respectively, as well as Si-O-Si bending and symmetric stretching vibrations. Raman shift in the 950–1000  $\text{cm}^{-1}$  region results from structural components of metasilicate. The network that develops in the current glasses as a result of the modifying

action of  $K^+$ ,  $Ca^{2+}$ , and  $Mg^{2+}$  may easily accommodate the formation of their respective metasilicate units. These units are less strong than disilicate units, where two silicate tetrahedra share oxygen more evenly. Near  $1080\text{ cm}^{-1}$ , disilicate units exhibit Raman bands at substantially higher wave numbers [6]. Bands about  $1100\text{ cm}^{-1}$  are caused by Si-O-Si links vibrating asymmetrically. A vibration in which the bridging oxygen ions travel counterclockwise to their Si neighbors is responsible for the band seen at about  $1055\text{ cm}^{-1}$  [7]. The oxygen ions travel roughly at a right angle to the Si-Si lines and in the Si-O-Si planes in the band at around  $800\text{ cm}^{-1}$ , which is referred to as a "bond-bending" motion. The modes are no longer believed to be confined at lower frequencies; hence the peaks are not as well defined. The  $SiO_4$  tetrahedron without non-bridging oxygen ions, however, may be recognized by the high peaks at  $495\text{ cm}^{-1}$  and  $435\text{ cm}^{-1}$  in CM-0, CM-20, and CM-30. According to the glass spectra, all of these glasses have  $SiO_4$  tetrahedra with one non-bridging oxygen ion as their primary structural unit, which is similar to that found in disilicate oxides. Glass containing CaO has a small peak at  $950\text{ cm}^{-1}$  in its spectrum that indicates the existence of  $SiO_4$  tetrahedra with two non-bridging oxygen ions. Glass-ceramics with MgO contents greater than 20 wt% ceased to exhibit shoulders between  $1416$  and  $1524\text{ cm}^{-1}$ . Particularly in high MgO content glass-ceramics, the band position at  $1427$ ,  $1659$ , and  $1758\text{ cm}^{-1}$  gets sharper. The Raman peaks become sharp with heat treatment duration and MgO content in the glasses. The Raman results are supported by the XRD results. As the crystallization increases the Raman peaks increase as shown in figures 4.2(a), (b), (c) and (d) [8-12].

### 4.3 UV analysis



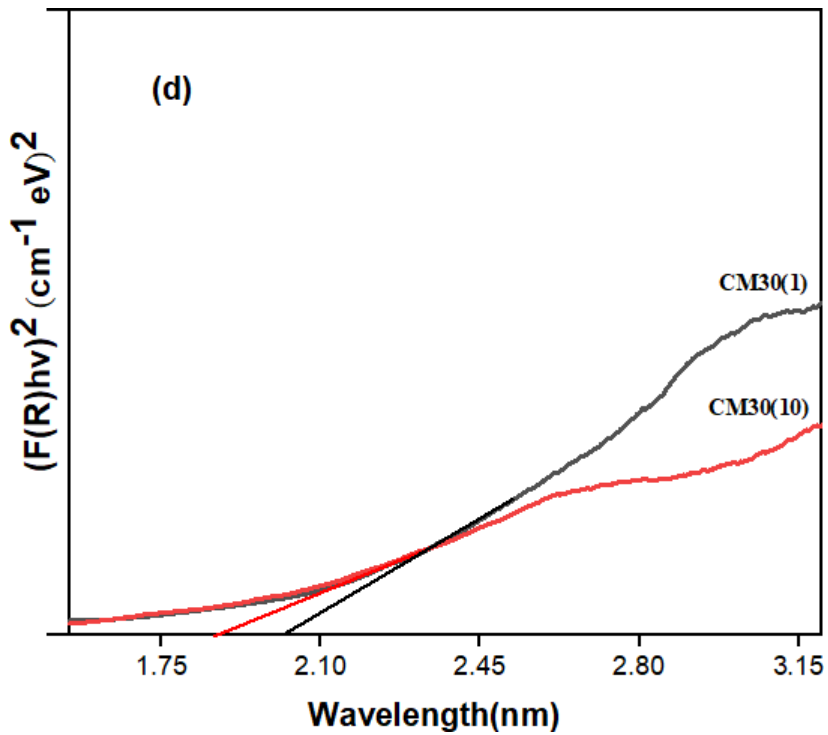
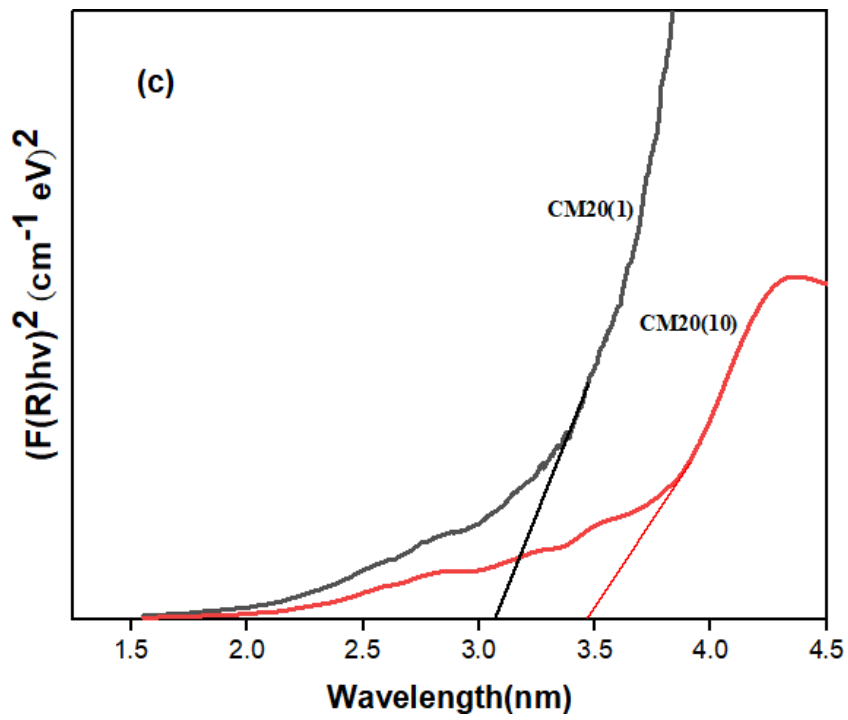


Figure 4.3 Tauc's plot for determination of optical band gap of glass-ceramics (a) CM-0 heat treated at 1hour and 10hour, (b) CM-10 heat treated at 1 hour and 10hour, (c) CM-20 heat treated at 1hour and 10hour, (d) CM-30 heat treated at 1 hour and 10hour.

Table 4.2 Band gap values of given glass ceramics with their sample code

Sample Code	Band Gap (eV)
CM0(1)	3.40
CM0(10)	3.80
CM10(1)	3.54
CM10(10)	3.58
CM20(1)	3.07
CM20(10)	3.46
CM30(1)	2.02
CM30(10)	1.87

Figure 4.3 (a), (b), (c) and (d) show the optical band gap of all heat-treated samples. The extrapolation of curves linear regions yields the optical band gap energies. In Table 4.2, the optical band gap values are also listed. The optical band gap is not showing any trend. The highest band gap is observed in CM0(10) glass ceramics. The lowest optical band gap is observed in CM30 (10) glass ceramics. Another salient feature is the optical band increases as the crystallization except CM 30 glass ceramics. Interestingly, these glass ceramics only contain Mg related crystalline phases. These particular glass ceramic exhibit K<sub>2</sub>MgSiO<sub>4</sub> phase apart from MgSiO<sub>4</sub> and CaMgSiO<sub>4</sub> crystalline phases. It may be related to the band gap of K<sub>2</sub>MgSiO<sub>4</sub> phase. Overall, the typical band gap variations in the glass ceramics depends on the evolution of the different crystalline phases and their chemical nature [13-16]. The optical band gap is found to be increasing in case of CM-0 and CM-10 glass ceramics where the concentration of CaO is greater than MgO. But on the other hand, the value of optical band gap is found to be decreasing for CM-20 and CM-30 glass-ceramics which has concentration of MgO greater than CaO. This is due to the fact that Mg<sup>2+</sup> has a smaller radius and greater polarizability than Ca<sup>2+</sup>, which causes it to induce more charge on NBOs, reducing the ionic character of oxygen ions, lowering the top of the valence band, and raising

the optical band gap. Additionally, it is widely known that switching a lighter element for a heavier one reduces the optical band gap and vice-versa. When a heavier metal is introduced, the Si-O-Si bond is broken, resulting in the development of NBOs, which has a higher negative charge than the bridging oxygen and increases the ionic character [17].

## References

- [1] A.M. Hofmeister, J.E. Bowey, *Mon. Not.R. Astron. Soc* 367 (2006)577.
- [2] N. Lahl, D. Bahadur, K. Singh, L. Singheiser, K. Hilpert, *J. Electrochem. Soc.* 149 (5) (2002)A607.
- [3] N. Zotov, E. Ebbsjo, D. Timpel, H. Keppler, *Phys. Rev. B* 60 (1999)6383.
- [4] V.P. Zakaznova-Herzog, W.J. Malfait, F. Herzog, W.E. Halter, *J. Non-Cryst. Solids* 353 (2007)4015.
- [5] M. Wang, J. Cheng, M. Li, F. He, *Physica B: Condens. Matter* 406 (2011)3865.
- [6] A.G. Kalampounias, *Bull. Mater. Sci.* 34 (2011) 299.
- [7] B.O. Mysen, L.W. Finger, D. Virgo, F.A. Seifert, *Am. Mineral* 67 (1982)686.
- [8] P. Mcmillan, *Am. Mineral* 69 (1984) 622.
- [9] A. K. Yadav, C.R. Gautam, A. Gautam, V. K. Mishra, *Phase Trans.* 10 (2013)86.
- [10] Szumera, Magdalena. *Spectrochimica Acta Part A: Molecular and Biomolecular Spectroscopy* 130 (2014): 1-6.
- [11] Rim, Young Hoon, *J Non-CrystSolids* 500 (2018): 336-344.
- [12] Muniz, R. F., *Ceram Int* 47.17 (2021): 24966-24972.
- [13] Wang, Huili, *Ceram Int* 47.9 (2021): 12276-12283.
- [14] Zhang, YuXuan, et al *JNon-CrystSolids* 563 (2021): 120701.
- [15] J. Tauc, *Mater. Res. Bull.* 5 (1970)721.
- [16] C. Rajyasree, D.K. Rao, *J. Non-Cryst. Solids* 357 (2011)836.
- [17] G. Kaur, O.P. Pandey, K. Singh, *J. Non-Cryst. Solids* 358 (2012) 2589

**5.1 Conclusion**

Four potassium silicate with variable calcium and magnesium oxides were heat treated at 850°C for 1 and 10 hours to convert into glass ceramics. After 1 hour heat treatment, the higher MgO (30mol%) in 55SiO<sub>2</sub>-10K<sub>2</sub>O-5MgO-30MgO containing glasses converted in glass ceramics and form the Mg<sub>2</sub>SiO<sub>2</sub> phases. The MgO content instead of CaO in the present glasses promote the crystallization MgO content also prevent the SiO<sub>2</sub> phase formation. The optical band gap donot show any trend since the formation of different crystalline phases. However, the volume fraction of crystallization is high in higher MgO contained glasses. The glass ceramics exhibit the higher band than glasses except CM-30 glass ceramics. The Raman spectra show the remarkable change as glass converted into the glass ceramics and Raman peaks become sharper. The optical band gap is observed in wide band gap semiconductor range.

**5.2 Future scope**

The heat treatment duration could be increased to study the effect of volume fraction of different crystalline phases on various properties. The prevention of SiO<sub>2</sub> phase in high content of MgO containing glass could be use as glass salient in solid oxide fuel cells.

## Turnitin Originality Report

Processed on: 28-Jul-2022 13:56 IST  
 ID: 1876128702  
 Word Count: 6523  
 Submitted: 1

Jasleen Thesis By Jasleen Kaur

Similarity Index

14%

Similarity by Source

Internet Sources:	8%
Publications:	9%
Student Papers:	4%

3% match (Internet from 12-Oct-2021)

<http://tudir.thapar.edu:8080/jspui/bitstream/10266/4922/4/4922.pdf>

2% match (student papers from 17-Jun-2017)

[Submitted to Thapar University, Patiala on 2017-06-17](#)

1% match (publications)

[M. Leśniak, J. Partyka, K. Pasiut, M. Sitarz. "Microstructure study of opaque glazes from SiO<sub>2</sub>-Al<sub>2</sub>O<sub>3</sub>-MgO-K<sub>2</sub>O-Na<sub>2</sub>O system by variable molar ratio of SiO<sub>2</sub>/Al<sub>2</sub>O<sub>3</sub> by FTIR and Raman spectroscopy". Journal of Molecular Structure, 2016](#)

1% match (publications)

[Leibo Deng, Xuefeng Zhang, Mingxing Zhang, Xiaolin Jia. "Effect of CaF<sub>2</sub> on viscosity, structure and properties of CaO-Al<sub>2</sub>O<sub>3</sub>-MgO-SiO<sub>2</sub> slag glass ceramics". Journal of Non-Crystalline Solids, 2018](#)

1% match (publications)

[Praveen Jha, Satwinder Singh Danewalia, Gaurav Sharma, K. Singh. "Antimicrobial and bioactive phosphate-free glass-ceramics for bone tissue engineering applications". Materials Science and Engineering: C, 2018](#)

1% match (publications)

[S.J. Watts, R.G. Hill, M.D. O'Donnell, R.V. Law. "Influence of magnesia on the structure and properties of bioactive glasses". Journal of Non-Crystalline Solids, 2010](#)

< 1% match (Internet from 25-Jun-2022)

<https://tudir.thapar.edu:8080/jspui/bitstream/10266/5741/1/Thesis%201.5%20spacing.pdf>

< 1% match (student papers from 28-Nov-2015)

[Submitted to Thapar University, Patiala on 2015-11-28](#)

< 1% match (student papers from 16-Jun-2017)

[Submitted to Thapar University, Patiala on 2017-06-16](#)

< 1% match (student papers from 17-Jul-2018)

[Submitted to Thapar University, Patiala on 2018-07-17](#)

< 1% match (publications)

[Young Hoon Rim, Mac Kim, Jae-Hyeon Ko, Yong Suk Yang. "Influence of ionic radius of alkaline-earth metals in ion conducting 2\(Ca, Sr, Ba\)O 2TiO<sub>2</sub>SiO<sub>2</sub> glasses". Journal of Non-Crystalline Solids, 2018](#)

*Jasleen Kaur*

*dsb*